Short communication

Export of ^{13}C-depleted dissolved inorganic carbon from a tidal forest bordering the Amazon estuary

Gwenaël Abril [a,*], Jonathan Deborde [a], Nicolas Savoye [a], Francine Mathieu [a], Patricia Moreira-Turcq [b], Felipe Artigas [c], Tarik Meziane [d], Luis Roberto Takiyama [e], Márcio S. de Souza [e], Patrick Seyler [b]

[a] Laboratoire EPOC, Environnements et Paléoenvironnements Océaniques et Continentaux, Université de Bordeaux, CNRS, UMR, 5805 Bordeaux, France
[b] Laboratoire GET, Géosciences et Environnement de Toulouse, Institut de Recherche pour le Développement, Université Paul Sabatier, Toulouse, France
[c] Laboratoire d'Océanologie et Géosciences, CNRS, Université du Littoral Côte d'Opale, Wimereux, France
[d] Laboratoire BOREA, UMR 7208, Département Milieux et Peuplements Aquatiques, Muséum National d'Histoire Naturelle, Paris, France
[e] Instituto de Pesquisas Científicas e Tecnológicas do estado do Amapá — IEPA, Macapá, AP, Brazil

ARTICLE INFO

ABSTRACT

Tidal wetlands play a significant role in the coastal carbon cycle and exchange material with the atmosphere and coastal ocean. Here, we report on changes in dissolved inorganic carbon speciation and isotopic composition throughout a 24 h cycle (2 tidal cycles) in Feb. 2007 in a channel connecting the Amazon estuary to the basin of a tidal forest. At this site, tropical forest soils are inundated at high tide by estuarine freshwater, and temporal concentration changes in the channel reflect exchanges between the forest and estuary. Our data show an export of dissolved inorganic carbon (DIC) in the form of excess CO_2 and, to a much lesser extent, CH_4. However, the tidal forest traps suspended sediments. Mixing plots of DIC versus conductivity showed that the DIC originated from the tidal forest soil, with a negligible contribution from the local watershed. Evolution of the isotopic signature of DIC reveals a ^{13}C-depleted source ($-56.9 \pm 3.3‰$), presumably originating from a dominant methanogenic pathway of carbon mineralization followed by almost complete CH_4 oxidation in the organic clay-rich freshwater soil.

1. Introduction

During the last two decades, the scientific community has progressively recognized the significant role of the coastal zone in the global carbon cycle (Wollast, 1998; Borges, 2005; Cai, 2011). Coastal ecosystems intensively process organic material carried by rivers and deeply modify its nature and quantity as it transits through the land–sea interface. Many works have described estuaries as filters of terrestrially derived material, as having a net heterotrophy and by the fact that almost all of them degas CO_2 to the atmosphere (Frankignoulle et al., 1998; Cai et al., 1999; Abril et al., 2000, 2002; Cai, 2011; Borges and Abril, 2011). Coastal ecosystems also produce their own organic matter that can be further consumed, buried, exported or mineralized (Gattuso et al., 1998; Nérot et al., 2009; Duarte et al., 2010). Borges (2005) has emphasized the heterogeneity of the coastal zone in terms of its metabolic balance and atmospheric CO_2 exchanges, which are different in

estuaries, lagoons, seagrass meadows, upwelling, and shelves. Before precisely quantifying CO_2 fluxes in this coastal mosaic, there is a need to develop an objective conceptualization of carbon flows through each type of ecosystem to generate adequate field methodologies and build operational sub-models. Intertidal areas are particularly dynamic and complex sub-systems of the coastal zone (Cai, 2011). During emersion, primary production is favored under optimal light conditions, and the large variety of vegetation and benthic algae is able to uptake CO_2 directly from the atmosphere (Kathilankal et al., 2008; Polsenaere et al., 2012). Conversely, regular tidal water movements enhance the lateral exchange of solutes and particles with adjacent coastal seas (Wang and Cai, 2004; Bouillon et al., 2007). It has been shown that saltmarshes and mangroves export dissolved inorganic carbon (Cai et al., 1999, 2003; Neubauer and Anderson, 2003; Borges et al., 2003; Wang and Cai, 2004; Bouillon et al., 2007; Cai, 2011; Borges and Abril, 2011). Here, we confirm this export from a hitherto undocumented intertidal ecosystem: tropical tidal forests that border the freshwater region of the Amazon estuary. In contrast to other documented systems, the carbon export of these tropical tidal forests occurred mainly in the form of excess CO_2 and not as

* Corresponding author.
E-mail address: g.abril@epoc.u-bordeaux1.fr (G. Abril).

carbonate alkalinity. The carbon export was also unexpectedly ^{13}C-depleted.

2. Methods

At the mouth of the Amazon River (Fig. 1A), freshwater is not diluted with seawater; tidal amplitudes range between 2 and 3.5 m and predominate year-round over changes in the water level resulting from river discharge (Kosuth et al., 2009). This estuarine region is bordered by an extensive area of flooded forest, which is composed of widely diverse tropical plants that tolerate flooding (notably palms) (Takiyama et al., 2006). This tidal forest can reach 10 km wide at each edge of the river and on islands. In this area, the sedimentary surface of the forest and open savannah that is flooded twice a day by the tide is similar to that of the open waters in the Amazon channel. The volume of water flooding the forest is presumably minor, due to a maximum water depth of 1–3 m in the wetland compared to ∼40 m in the main channels. In Feb. 2007, we conducted a 24 h experiment at a single station in a channel connecting the Amazon estuary to a 22 km^2 basin of tidal forest. Freshwater was continuously pumped to a WTW thermoconductimeter and a marble-type equilibrator (Frankignoulle et al., 2001; Abril et al., 2006) connected to a LICOR® 820 Infra-Red Gas Analyzer, which was calibrated before and after the

Fig. 1. Map of the study site and sampling locations; S24 is the station where the 24-h sampling was performed (S 0 15′ 12″; W 51 45′ 27″); SU is the station representative for upstream, watershed waters that were sampled at low tide; SC is the station sampled in the Amazon main channel. The shaded area delineates the sampled tidal basin.

cruise; data were recorded every 1 min. Precision was evaluated at ±15 ppmv in the 0–10,000 ppmv range. Water was sampled every hour and transferred to duplicate 150 mL serum vials that were poisoned with $HgCl_2$ (1 mg L^{-1} final concentration), sealed and transported to the laboratory for the determination of the methane concentration and isotopic composition of dissolved inorganic carbon (δ^{13}C-DIC). CH_4 was measured by gas chromatography as described in Abril et al. (2007) and δ^{13}C-DIC by EA-IRMS following the protocol of Bouillon et al. (2007). Repeatability was ±10 nM and ±0.1‰ for CH_4 and δ^{13}C-DIC, respectively. Water was also filtered through pre-combusted and pre-weighed 0.7 μm glass fiber filters. The filters were dried at 60 °C for the gravimetrical determination of total suspended solids (TSS). After carbonate removal with 0.1 N HCl, particulate organic carbon (POC) was measured with a LECO® elemental analyzer (repeatability ±0.1% TSS). Water filtrates were kept cool until the analysis of total alkalinity (TA) was performed in the laboratory by means of gran titration with 0.1 N HCl (repeatability ±5 μmol L^{-1}). Dissolved inorganic carbon (DIC) was calculated as the sum of the measured TA and the CO_2 concentration deduced from the measured pCO_2 and the solubility coefficient of CO_2 from Weiss (1974). We assumed that the carbonate ion concentration was zero and that the bicarbonate concentration equaled that of TA because the in situ pH was between 6.7 and 7.2. In this pH range, the underestimation of DIC calculated that way compared to the one calculated from dissociation constants is less than 0.2%. At low tide, during the experiment, we sailed ∼20 km upstream in the shallow channel with a small boat until we could find water with a significantly lower conductivity, which was assumed to be representative for watershed waters and not affected by the Amazon flooding. Finally, the Amazon estuary end-member was sampled the same way: at the center of the main stem, just in front of the tidal forest, at high and low tides.
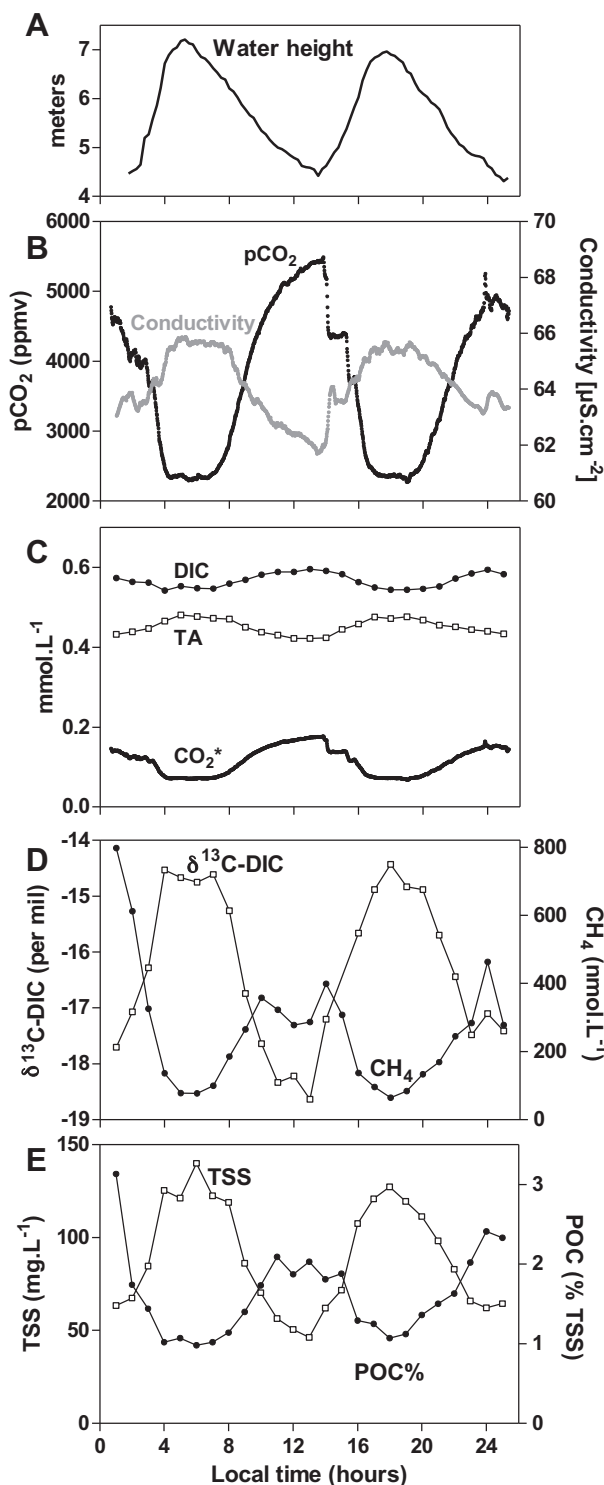
3. Results and discussion

All parameters varied significantly over a 24 h period and were well synchronized with the two tidal cycles whose amplitude was 2.6 m (Fig. 2A). pCO_2, DIC, CH_4 and the POC content of TSS had maximum values at low tide and minimum values at high tide. Inversely, conductivity, TA, δ^{13}C-DIC and the POC content of TSS had maximum values at high tide and minimum values at low tide (Fig. 2B–E). Conductivity only changed by 6% and ranged from 62 to 66 μS cm^{-1}, which were very close to the values measured in the Amazon main stem. pCO_2 at low tide was 5000 ± 300 ppmv, which was more than twice the high tide value of 2320 ± 40 ppmv (Fig. 2B); the high tide value was also observed in the Amazon main stem. These tidal pCO_2 patterns are consistent with the observations in saltwater intertidal systems, with the pCO_2 ranges being similarly elevated in some mangrove creeks (Borges et al., 2003; Bouillon et al., 2007) but reduced in temperate saltmarshes (Wang and Cai, 2004). Although TA showed a slight trend that was opposite to that of pCO_2, the calculated DIC concentrations were still higher at low tide than at high tide, showing an export from the tidal forest mostly in the form of dissolved CO_2 (Fig. 2C). Dissolved CO_2 was 13% of the DIC in Amazon waters at high tide but was 29% in the waters flowing from the tidal forest at low tide. The δ^{13}C-DIC values of −14 ± 0.2‰ at high tide as well as in the Amazon main stem were comparable to the range (−16 to −12.5‰) observed at Obidos, located 550 km upriver (Quay et al., 1992), but were slightly more negative than the value (−11‰) observed 50 km downriver in October 1991 (Druffel et al., 2005). δ^{13}C-DIC values of −18 ± 0.5‰ at low tide revealed a ^{13}C-depleted source in the tidal forest. CH_4 followed the same trend as CO_2 and was tidally exported from the forest to the estuary. Finally, the forest acted as a trap for suspended sediments, as the TSS concentrations were 2.5 times lower at low
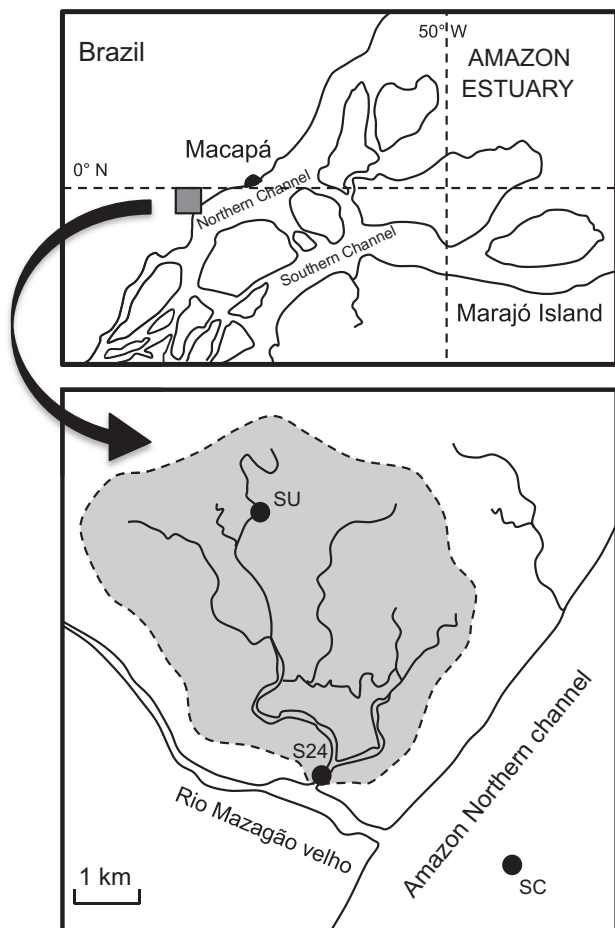
tide than at high tide (Fig. 2E). However, suspended particles were enriched in the POC at low tide relative to high tide (Fig. 2E), suggesting a flushing of coarse litter debris from the forest soil. The POC concentrations expressed in mg L^{-1} (not shown) were fairly constant throughout the cycle, suggesting that the trapping of

Fig. 2. Time course of parameters throughout the two tidal cycles. A: water height; B: water pCO$_2$ and conductivity as recorded every minute; C: the DIC, TA (HCO$_3^-$) and CO$_2$ concentrations (mmol L^{-1}) recorded every hour (the DIC and TA) and minute (CO$_2$); D: the δ^{13}C-DIC (versus PDB) and CH$_4$ concentration (nmol L^{-1}); E: Total Suspended Solids (mg L^{-1}) and the weight percentage of the POC in the TSS (%).
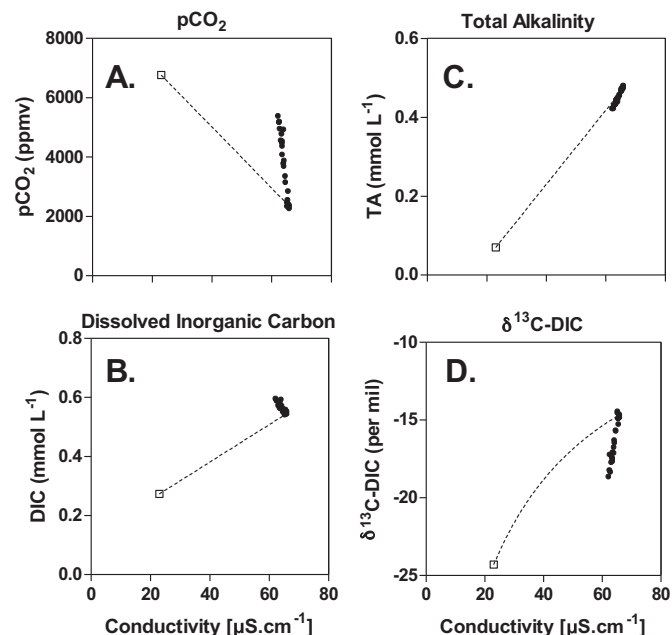
Fig. 3. Mixing plot of the pCO$_2$, TA, DIC and δ^{13}C-DIC versus conductivity; the white squares correspond to the watershed waters that were collected from the most upstream channel at low tide; black dots correspond to variations throughout the tidal cycle at the outlet of tidal basin.

organic carbon bound to Amazon mineral particles was compensated for by the mobilization of fresh material from the forest soil.

The decrease in conductivity at low tide was small but significant and resulted from a small dilution from local watershed inputs. Measured conductivity in the channel farthest upstream of the tidal basin at low tide was 23 μS cm^{-1}. Assuming conservative mixing between this water and the Amazon, this conductivity corresponds to a contribution of 9% of water from the local watershed at the experimental site, only at low tide. Plotting the parameters of dissolved inorganic carbon versus conductivity showed a conservative behavior for the TA only, whereas the pCO$_2$ and calculated DIC were well above the mixing lines, and the δ^{13}C-DIC was well below (Fig. 3). This confirms that mixing with waters from the local watershed is quantitatively a very minor DIC source and that the large amounts of the DIC and CO$_2$ exported from the tidal basin originates from microbial and root respiration in the flooded forest soil. This conclusion is similar to those drawn from saltmarshes and mangroves, except that the latter environments exported the DIC primarily in the form of carbonate alkalinity (Borges et al., 2003; Wang and Cai, 2004) as a result of dominant sulfate reduction, which is a proton consuming process in marine sediments (Table 1; Hu and Cai, 2011). Here, the δ^{13}C-DIC was negatively correlated to

Table 1
Idealized stoichiometry of reactions discussed in this paper; all reactions have been expressed without protons to describe their impact on the carbonate system. Sulfate reduction is assumed to be dominant in marine sites and produces more carbonate alkalinity than free CO$_2$, whereas the methanogenic/methanotrophic pathway predominates in freshwater sites and produces isotopically light CO$_2$.

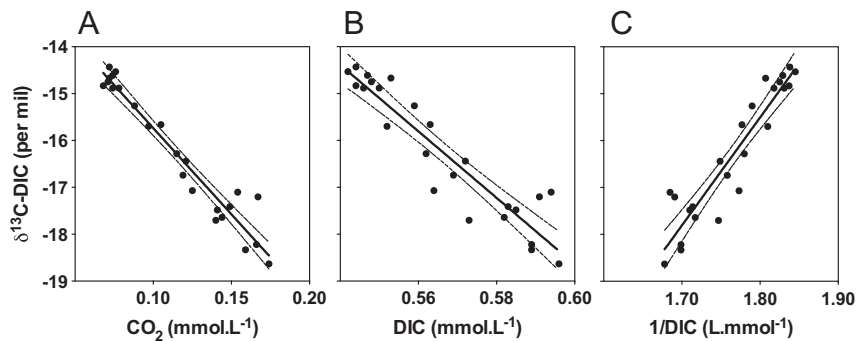| Sulfate reduction | at pH < 7 | $2CH_2O + SO_4^{2-} \rightarrow 2HCO_3^- + H_2S$ |
	at pH > 7	$2CH_2O + SO_4^{2-} \rightarrow CO_2 + HCO_3^- + H_2O + HS^-$
Fermentative methanogenesis		$2CH_2O \rightarrow CO_2 + CH_4$
Bacterial CO$_2$ reduction		$CO_2 + 8H_2 \rightarrow CH_4 + 2H_2O$
Aerobic methane oxidation		$CH_4 + 2O_2 \rightarrow CO_2 + 2H_2O$

Fig. 4. Correlation between the δ^{13}C-DIC and A: the CO_2 concentration; B: the DIC concentration; C: 1/DIC; allowing isotopic mass balance calculation.

the CO_2 concentration and the calculated DIC concentration and positively correlated to the inverse of the DIC concentration (Fig. 4). The δ^{13}C of the added DIC ($\delta^{13}C_{added}$) can be deduced either as the A term from a first polynomial relationship, δ^{13}C-DIC = A + B/DIC (Bouillon et al., 2007), or by considering a simple conservative mixing between two sources, i.e., the Amazon freshwater estuary and the tidal forest soil; in this case, the DIC added to the waters between the high tide and the low tide is likened to the DIC concentrations and isotopic composition observed between these two end-members by a mass balance equation:

$$\delta^{13}C_{added} = \frac{DIC_{HT}\delta^{13}C_{HT} - DIC_{LT}\delta^{13}C_{LT}}{DIC_{HT} - DIC_{LT}}$$

where $\delta^{13}C_{HT}$ and $\delta^{13}C_{LT}$ refer to the isotopic composition of DIC at high and low tide, respectively, and DIC_{HT} and DIC_{LT} refer to their respective concentrations. The first method results in a $\delta^{13}C_{added}$ of $-56.9 \pm 3.3‰$, whereas the second method gives consistent $\delta^{13}C_{added}$ values between -48 and $-63‰$ according to the assumed values for the end-members. Accounting for gas exchange and ^{13}C equilibration with the atmosphere, which may have occurred between soil pore waters and drainage channels, would lead to an even more depleted value of $\delta^{13}C_{added}$ (Polsenaere and Abril, 2012). This $\delta^{13}C_{added}$ value is extremely negative in comparison with the signature of the organic C potential source in a forest dominated by C3 plants. It suggests that a significant fraction of the CO_2 exported from the flooded forest soil originates from the oxidation of methane, which is the only quantitatively significant form of carbon that could potentially be so ^{13}C-depleted. However, there are several unknown variables in the processes that could result in such a release of ^{13}C-depleted CO_2 and these deserve a deeper investigation and include soil and pore water sampling. The bacterial reduction of CO_2 and/or the fermentation of methylated substrates produce strongly ^{13}C-depleted CH_4, but they yield ^{13}C-enriched CO_2 in anoxic sediments (Whiticar, 1999; Hornibrook et al., 2000). To reach these ^{13}C-depleted values in surface waters, CO_2 must result from the fast oxidation of CH_4 that would be preferentially transported relative to ^{13}C-enriched CO_2 from deep anoxic soil. The mobilization and re-dissolution of methane bubbles may occur with tidal changes in hydrostatic pressure and these play an important role (Borges and Abril, 2011). The enhancement of microbial oxidation in the presence of fine suspended particles (Abril et al., 2007) could then occur only in the oxic surface waters and would result in the observed export of ^{13}C-depleted DIC.

Our observations in the Amazon estuary revealed that freshwater tidal forests export the DIC to surrounding waters in a manner similar to that of saltmarshes and mangroves. This export was driven by an influx of soil pore waters from so-called "tidal pumping" (Borges et al., 2003). However, the composition of this DIC is fundamentally different in the two types of environments,

as it is the result of different predominant pathways of CO_2 production (Table 1). In saline environments, sulfate reduction predominates as the major pathway for sedimentary organic matter degradation and produces in majority bicarbonates (Hu and Cai, 2011). As a result, in saltmarshes and mangroves, tidal pumping exports the DIC mainly in the form of carbonate alkalinity (Neubauer and Anderson, 2003; Borges et al., 2003; Bouillon et al., 2007; Cai, 2011). Using a similar sampling strategy in a Tanzanian mangrove, Bouillon et al. (2007) found that the isotopic signature of the added DIC was $-22‰$ and this was consistent with the signature of the POC eroded from the mangrove soils. This signature is also consistent with the predominance of sulfate reduction in saline tidal wetlands, where potentially little isotopic fractionation is occurring (Boehme et al., 1996). In contrast, under freshwater conditions such as those at our study site, methanogenesis from CO_2 and from acetate (Table 1) may become the predominant pathway for sedimentary organic matter mineralization and result in a strong isotopic fractionation, leading to the produced methane being ^{13}C-depleted (Whiticar, 1999). Our results suggest that most of this methane is then oxidized to CO_2, as the observed CO_2 concentrations throughout the experiment were $200-1000$ times higher than the CH_4 concentrations (Fig. 2). Very small amounts of CH_4 were exported by tidal pumping in comparison with CO_2. Low salinity and high turbidity regions of estuaries are environments that are favorable for enhanced CH_4 oxidation (Abril et al., 2007). A significant contribution by methane oxidation to the CO_2 released from soil is the only way to explain the ^{13}C-depletion of the exported DIC and is also consistent with an export in the form of excess CO_2 rather than bicarbonates (Table 1). Assuming the tidal forest extends over an average width of 3 km and a length of 300 km and has an average water depth of 1 m (Takiyama et al., 2006), the volume of water exchanged during each tidal cycle of 13 h is 0.9 billion m^3. This amount corresponds to 19230 m^3 s^{-1}, which is 7% and 24% of the maximum and minimum discharge of the Amazon River, respectively. These water fluxes may explain why our data, and those from previous reports (Druffel et al., 2005), do not provide clear evidence of a significant depletion in the ^{13}C-DIC signatures in the main stem, due to export from the tidal forest.

References

Abril, G., Nogueira, M., Etcheber, H., Cabeçadas, G., Lemaire, E., Brogueira, M.J., 2002. Behaviour of organic carbon in nine contrasting European estuaries. Estuarine, Coastal and Shelf Science 54, 241–262.

Abril, G., Richard, S., Guérin, F., 2006. In-Situ measurements of dissolved gases (CO_2 and CH_4) in a wide range of concentrations in a tropical reservoir using an equilibrator. Science of the Total Environment 354, 246–251.

Abril, G., Commarieu, M.-V., Guérin, F., 2007. Enhanced methane oxidation in an estuarine turbidity maximum. Limnology and Oceanography 52, 470–475.

Abril, G., Etcheber, H., Borges, A.V., Frankignoulle, M., 2000. Excess atmospheric carbon dioxide transported by rivers into the Scheldt Estuary. Comptes Rendus Géosciences Série IIA 330, 761–768.

Boehme, S., Blair, N., Chanton, J.P., Marteens, C.A., 1996. A mass balance of ^{13}C and ^{12}C in an organic-rich methane-producing marine sediment. Geochimica et Cosmochimica Acta 60, 3835–3848.

Borges, A.V., Abril, G., 2011. Carbon Dioxide and Methane Dynamics in Estuaries in Treatise on Coastal and Estuarine Science. In: Biogeochemistry, vol. 8. Elsevier, pp. 119–161.

Borges, A.V., 2005. Do we have enough pieces of the jigsaw to integrate CO_2 fluxes in the coastal ocean? Estuaries 28, 3–27.

Borges, A.V., Djenidi, S., Lacroix, G., Théate, J., Delille, B., Frankignoulle, M., 2003. Atmospheric CO_2 flux from mangrove surrounding waters. Geophysical Research Letters 30 (11), 1558. http://dx.doi.org/10.1029/2003GL017143.

Bouillon, S., Middelburg, J.J., Dehairs, F., Borges, A.V., Abril, G., Flindt, M.R., Ulomi, S., Kristensen, E., 2007. Importance of intertidal sediment processes and porewater exchange on the water column biogeochemistry in a pristine mangrove creek (Ras Dege, Tanzania). Biogeosciences 4, 311–322.

Cai, W.-J., Pomeroy, L.R., Moran, M.A., Wang, Y.C., 1999. Oxygen and carbon dioxide mass balance for the estuarine-intertidal marsh complex of five rivers in the southeastern US. Limnology and Oceanography 44 (3), 639–649.

Cai, W.-J., Wang, Z.H.A., Wang, Y.C., 2003. The role of marsh-dominated hetero-trophic continental margins in transport of CO_2 between the atmosphere, the land-sea interface and the ocean. Geophysical Research Letters 30 (16), 1849. http://dx.doi.org/10.1029/2003GL017633.

Cai, W.-J., 2011. Estuarine and coastal ocean carbon paradox: CO_2 sinks or sites of terrestrial carbon incineration? Annual Review of Marine Science 3, 123–145 http://dx.doi.org/10.1146/annurev-marine-120709-142723.

Duarte, C.M., Marba, N., Gacia, E., Fourqurean, J.W., Beggins, J., Barron, C., Apostolaki, E.T., 2010. Seagrass community metabolism: assessing the carbon sink capacity of seagrass meadows. Global Biogeochemical Cycles 24, 1–8.

Druffel, E.R.M., Bauer, J.E., Griffin, S., 2005. Input of particulate organic and dissolved inorganic carbon from the Amazon to the Atlantic Ocean. Geochemistry Geophysics and Geosystems 6, Q03009. http://dx.doi.org/10.1029/2004GC000842.

Frankignoulle, M., Borges, A.V., Biondo, R., 2001. A new design of equilibrator to monitor carbon dioxide in highly dynamic and turbid environments. Water Research 35 (5), 1344–1347.

Frankignoulle, M., Abril, G., Borges, A., Bourge, I., Canon, C., Delille, B., Libert, E., Théate, J.-M., 1998. Carbon dioxide emission from European estuaries. Science 282 (5388), 434–436.

Gattuso, J.-P., Frankignoulle, M., Wollast, R., 1998. Carbon and carbonate metabolism in coastal aquatic ecosystems. Annual Review of Ecology and Systematics 29, 405–434.

Hu, X., Cai, W.-J., 2011. An assessment of ocean margin anaerobic processes on oceanic alkalinity budget. Global Biogeochemical Cycles, GB3003. http://dx.doi.org/10.1029/2010GB003859.

Hornibrook, E.R.C, Longstaffe, E.J., Fyfe, W.S., 2000. Evolution of stable carbon isotope compositions for methane and carbon dioxide in freshwater wetlands and other anaerobic environments. Geochimica Cosmochimica Acta 64, 1013–1027.

Kathilankal, J.C., Mozdzer, T.J., Fuentes, D., D'Odorico, P., McGlathery, K.J., Zieman, J.C., 2008. Tidal influences on carbon assimilation by a salt marsh. Environmental Research Letters 3, 1–6.

Kosuth, P., Callède, J., Laraque, A., Filizola, N., Guyot, J.-L., Seyler, P., Fritsch, J.-M., Guimarães, V., 2009. Sea-tide effects on flows in the lower reaches of the Amazon River. Hydrological Processes 23, 3141–3150.

Nérot, C., Meziane, T., Provost-Govrich, A., Rybarczyk, H., Lee, S.Y., 2009. Role of grapsid crabs, parasesarma erythrodactyla, in entry of mangrove leaves into an estuarine food web: a mesocosm study. Marine Biology 156 (11), 2343–2352.

Neubauer, S.C., Anderson, I.C., 2003. Transport of dissolved inorganic carbon from a tidal freshwater marsh to the York River estuary. Limnology and Oceanography 48 (1), 299–307.

Polsenaere, P., Abril, G., 2012. Modelling CO_2 degassing from small acidic rivers using water pCO$_2$, DIC and δ^{13}C-DIC data. Geochimica et Cosmochimica Acta 91, 220–239.

Polsenaere, P., Lamaud, E., Lafon, V., Bonnefond, J.-M., Bretel, P., Delille, B., Deborde, J., Loustau, D., Abril, G., 2012. Spatial and temporal CO_2 exchanges measured by Eddy correlation over a temperate intertidal flat and relations with net ecosystem production. Biogeosciences 9, 249–268.

Quay, P.D., Wilbur, D.O., Richey, J.E., Hedges, J.I., Devol, A.H., 1992. Carbon cycling in the Amazon River: implications from the δ^{13}C compositions of particles and solutes. Limnology and Oceanography 37, 857–871.

Takiyama, L.R., Silva, S.L.F., Silva, U.R.L., 2006. Atlas da zona costeira estuarine do estado do Amapa, ISBN 85-87794-11-6, p. 77.

Wang, Z., Cai, W.-J., 2004. Carbon dioxide degassing and inorganic carbon export from a marsh dominated estuary (the Duplin River): a marsh CO_2 pump. Limnology and Oceanography 49, 341–352.

Weiss, R.R., 1974. Carbon dioxide in water and seawater: the solubility of a non-ideal gas. Marine Chemistry 2, 203–215.

Wollast, R., 1998. Evaluation and comparison of the global carbon cycle in the coastal zone and in the open ocean. In: Brink, K.H., Robinson, A.R. (Eds.), 1998. The Global Coastal Ocean, vol. 10. John Wiley & Sons, New York, pp. 213–252.

Whiticar, M.J., 1999. Carbon and hydrogen isotope systematics of bacterial forma-tion and oxidation of methane. Chemical Geology 161, 291–314.